Supporting Information for

**Investigation of Noise at a Microelectrode During a Faradaic Reaction**

Kaden Wheeler[1], Joseph Gott[1], Brian Roehrich[1], Julia Chung[2], Kajal Kajal[1],

Jaroslaw Syzdek[3], Joao Hespanha[4], Lior Sepunaru[1]*

1 – Department of Chemistry and Biochemistry, University of California at Santa Barbara, Santa Barbara, CA 93106, United States

2 – Interdepartmental Program in Biomolecular Science and Engineering, University of California at Santa Barbara, Santa Barbara, CA 93106, United States

3 – Bio-Logic USA LLC, 9050 Executive Park Dr., Ste. 110C, Knoxville, Tennessee 37923, United States

4 – Electrical and Computer Engineering Department, University of California at Santa Barbara, Santa Barbara, CA 93106, United States

* Lior Sepunaru, sepunaru@ucsb.edu

**Table of Contents**


| | | |
|---|---|---|
| Figure S1 | Noise scales expectedly with sampling frequency | S3 |
| Table S1 | Experimental RC values from EIS | S4 |
| | Derivation of Equation 3 | S4-S6 |
| Table S2 | Extracted equivalent circuit values | S7 |
| Figure S2 | Cyclic Voltammograms of $Ru(NH_3)_6Cl_3$ and 2,2,6,6-tetramethylpiperidine-N-oxyl | S8 |
| Table S3 | Calculated diffusion coefficient for $[Ru(NH_3)_6Cl_3]$ | S9 |
| Table S4 | Calculated diffusion coefficient for TEMPO | S9 |
| Figure S3 | Noise comparison from RMSE and PSD | S10 |
| Figure S4 | Noise does not depend on electrolyte concentration | S11 |
| Figure S5 | Temperature effects on noise | S12 |
| Figure S6 | Noise does not trend with the concentration of maltose | S13 |
| Figure S7 | Noise generated by EC' is invariant of current | S14 |
| Figure S8 | Noise deviation from classical shot or thermal phenomena | S15 |
| Figure S9 | Charge transfer resistance is negligible at high redox probe concentrations | S16 |
| Table S5 | Impedance fit parameters for $[Ru(NH_3)_6Cl_3]$ | S17 |
| Table S6 | Impedance fit parameters for TEMPO | S17 |
| Table S7 | Impedance fit parameters for TEMPO and Maltose (EC') | S17 |

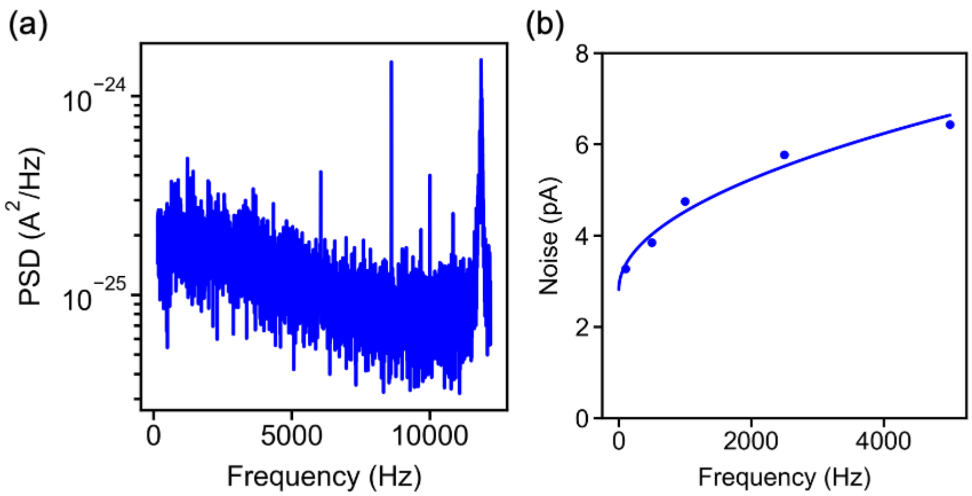


**Figure S1. Noise scales with the square root of the sampling frequency, as expected.** All measurements were done at a 1 MΩ resistor while varying the sampling frequency. (a) A power spectral density (PSD) of the resistor system measured at 25 kHz. (b) Noise at a resistor as a function of frequency (100 Hz – 5 kHz, blue) with a strong fit to $\sqrt{f}$ ($R^2 = 0.965$).

Note: Aliasing is a phenomenon that occurs when undersampling a signal, which introduces artifacts to the measured noise. The Biologic SP-300 potentiostat enables the measurement of the mean current, where multiple current measurements are averaged to one data point at the desired frequency, or the instantaneous current, where each measurement is taken at the desired frequency and sequentially recorded as a data point. In this work, we measure the mean current. The potentiostat samples as rapidly as it can (25 kHz) with a 50 kHz bandwidth and averages these data points into a single data point at the desired frequency (1 kHz). By sampling rapidly, more high-frequency signals are captured, reducing the impact of aliasing through limiting any signal distortion to only the higher frequencies.

**Table S1** Measured resistances and capacitances for each resistor from EIS circuit fitting.

| $\boldsymbol{R}$ (MΩ) | $\boldsymbol{C}$ (pF) |
|---|---|
| 0.67 | 0.68 |
| 1.03 | 1.32 |
| 2.23 | 0.83 |
| 8.15 | 0.68 |
| 10.50 | 0.56 |

**Derivation of Main Text Equation 3:**

There are three components of circuitry that must be considered (Figure 1c); (a) the measurement circuit, (b) the regulation noise equivalent circuit, and (c) the equivalent impedance of the measured resistor.

(a) The measurement circuit (Figure 1c – orange) has time constant $\tau_m = R_m C_m$. We consider this circuit to be ideal and that any potentiostatic noise will come from the regulation noise equivalent circuit. The key equation that must be considered for this case is then:

$$C_m \dot{V}_{C_m} = -\frac{V_{C_m}}{R_m} + I_z \qquad\qquad I_m = \frac{V_{C_m}}{R_m}$$

Where $I_Z$ is the current passing through the test impedance, $Z$ (Figure 1c – black) and $V_{C_m}$ is the voltage across the capacitor, $C_m$.

From which we conclude that:

$$\dot{I}_m = \frac{\dot{V}_{C_m}}{R_m} = -\frac{1}{C_m R_m} I_m + \frac{I}{C_m R_m} I_Z = -\frac{1}{\tau_m} I_m + \frac{1}{\tau_m} I_Z \qquad (1)$$

Where $I_m$ is the current passing through the measurement circuit.

It is important to emphasize that this equivalent circuit *models both the analog circuitry and any digital signal processing involved in the calculation of the current measurements.* Because of this, we should not expect the time constant $\tau_m$ to directly match that of the analog measurement circuit.

(b) The equivalent circuit for the noise induced by the reference electrode potential regulation system is composed of an RC loop with equivalent resistance $R_{eq}$ and capacitance $C_{eq}$, as well as a flat spectrum voltage source $V_{eq}(t) = \psi N_{eq}(t)$, where $\psi$ denotes a constant to be determined experimentally with units of $[\mathrm{V}/\sqrt{\mathrm{Hz}}]$ and $N_{eq}(t)$ denotes standard white noise with units of $\left[\sqrt{\mathrm{Hz}}\right]$, i.e.,

$$E\left[N_{eq}(t)\right] = 0 \left[\sqrt{\mathrm{Hz}}\right],\ R_{N_{eq}}(\tau) := E\left[N_{eq}(t) N_{eq}(t+\tau)\right] = \delta(\tau)\ [\mathrm{Hz}],$$

$$S_{N_{eq}}(f) \coloneqq \hat{R}_{N_{eq}}(f) = 1; \forall f,$$

where $R_{N_{eq}}(\tau)$ and $S_{N_{eq}}(f)$ denote the auto-correlation functions and power spectral density, respectively, of $N_{eq}(t)$.

In this case,

$$R_{V_{eq}}(\tau) \coloneqq E\left[V_{eq}(t)V_{eq}(t+\tau)\right] = \psi^2\delta(t)\ [\mathrm{V}^2] \Longrightarrow \hat{R}_{V_{eq}}(f) = \psi^2;\ \forall f\ [\mathrm{V}^2/\mathrm{Hz}]$$

$$\Rightarrow S_{V_{eq}}(f) \coloneqq \hat{R}_{V_{eq}}(f) = \psi^2 \qquad [\mathrm{V}^2/\mathrm{Hz}],$$

where $R_{V_{eq}}(\tau)$ and $S_{V_{eq}}(f)$ denote the auto-correlation functions and power spectral density, respectively, of the signal $V_{eq}(t)$.

While the spectrum of $V_{eq}(t)$ is flat, the spectrum of the voltage across the equivalent circuit is not flat, due to low pass filtering of the RC loop with time constant $\tau_{eq} = R_{eq}C_{eq}$. The key equation for this circuitry is

$$C_{eq}\dot{V}_{C_{eq}} = \frac{\psi N_{eq} - V_{C_{eq}}}{R_{eq}} + I_Z = -\frac{V_{C_{eq}}}{R_{eq}} + I_Z + \frac{\psi}{R_{eq}}N_{eq} \qquad (2)$$

(c) The test impedance $Z$ placed between the reference and working electrodes. In this case, we consider the impedance of the resistor measured from EIS, $R$, as well as the stray capacitance that is observed in our EIS, $C$. We consider the voltage across this RC parallel circuit to be $V_Z$.

Through the principle of superposition, we can analyze separately the two noise sources we consider (the thermal noise through our test impedance $Z$ and the noise from the regulation circuitry).

The thermal noise through the test impedance will be

$$C\dot{V}_Z = I_Z + \frac{\sqrt{2k_BTR}N_z - V_Z}{R} \Leftrightarrow C\dot{V}_Z = -\frac{V_Z}{R} + I_Z + \frac{\sqrt{2k_BTR}}{R}N_Z \qquad (3)$$

Where $N_Z$ denotes standard white noise, i.e., $S_{N_Z}(f) = 1, \forall f$.

For the noise through the regulation equivalent circuit, we have that $V_{C_{eq}} + V_Z + V_{C_m} = 0$ in the absence of a reference voltage. Therefore, we have that:

$$V_{C_{eq}} + V_Z + R_m I_m = 0, \qquad \dot{V}_{C_{eq}} + \dot{V}_Z + R_m\dot{I}_m = 0$$

We can then use this to eliminate $V_{C_{eq}}$ from Equations 1, 2, and 3 to conclude that:

$$\begin{bmatrix} \dot{V}_Z \\ \dot{I}_m \end{bmatrix} =$$

$$\begin{bmatrix} -\frac{C_{eq}R_{eq}R_m + R\tau_m + R_{eq}\tau_m}{CC_{eq}RR_{eq}R_m + CRR_{eq}\tau_m + C_{eq}RR_{eq}\tau_m} & \frac{C_{eq}R_{eq}R_m - R_m\tau_m}{CC_{eq}R_{eq}R_m + CR_{eq}\tau_m + C_{eq}R_{eq}\tau_m} \\ -\frac{CR - C_{eq}R_{eq}}{CC_{eq}\square\square R_{eq}R_m + CRR_{eq}\tau_m + C_{eq}RR_{eq}\tau_m} & -\frac{CR_{eq} + CR_m + C_{eq}R_{eq}}{CC_{eq}R_{eq}R_m + CR_{eq}\tau_m + C_{eq}R_{eq}\tau_m} \end{bmatrix} \begin{bmatrix} V_Z \\ I_m \end{bmatrix}$$

$$+ \begin{bmatrix} \frac{\sqrt{2k_BT}\left(C_{eq}R_m + \tau_m\right)}{\sqrt{R}\left(C\left(C_{eq}R_m + \tau_m\right) + C_{eq}\tau_m\right)} & -\frac{\tau_m\psi}{CC_{eq}R_{eq}R_m + CR_{eq}\tau_m + C_{eq}R_{eq}\tau_m} \\ -\frac{C_{eq}\sqrt{2k_BTR}}{CC_{eq}RR_m + CR\tau_m + C_{eq}R\tau_m} & -\frac{C\psi}{CC_{eq}R_{eq}R_m + CR_{eq}\tau_m + C_{eq}R_{eq}\tau_m} \end{bmatrix} \begin{bmatrix} N_Z \\ N_{eq} \end{bmatrix}$$

$$I_m = \begin{bmatrix} 0 & 1 \end{bmatrix} \begin{bmatrix} V_Z \\ I_m \end{bmatrix}$$

We can solve these matrices using the Lyapunov equation, which yields

$$\sigma_{Res}^2 = E[I_m^2] = \frac{k_BT\frac{R}{R^{\perp}}\left(\frac{R_{eq}C_{eq}R^{\perp}C^{\perp}}{RCR_mC_m} + 1\right) + \frac{1}{2}\left(\frac{RCR^{\perp}C^{\perp}}{R_{eq}C_{eq}R_mC_m} + 1\right)\frac{\psi^2}{R^{\perp}}}{(R + R_m)R_{eq}C_{eq} + \left(R_{eq} + R_m\right)RC + \left(R + R_{eq}\right)R_mC_m} \quad [\mathrm{A}^2]$$

Where

$$R^{\perp} \coloneqq R + R_{eq} + R_m \ [\Omega] \qquad C^{\perp} \coloneqq \frac{CC_mC_{eq}}{CC_{eq} + CC_m + C_mC_{eq}} \quad [\mathrm{F}]$$

Simply taking the square root of the variance yields the RMS equation of the noise through the resistor (Equation 3 main text). The resistances and capacitances for the elements from the potentiostat circuitry in Figure 1c that determined the plotted fit line were as follows.

**Table S2.** Equivalent impedances plugged into derived current noise equation

| Circuit Element | Equivalent Value and Units |
|---|---|
| $R_{eq}$ | 78 Ω |
| $C_{eq}$ | 30 pF |
| $\tau_m$ | 0.80 ms |
| $C$ | 0.65 pF |
| $\psi$ | 16 x $10^{-8}$ $\mathrm{V}/\sqrt{\mathrm{Hz}}$ |
| $C_m$ | 26 nF |
| $R_m$ | 31 kΩ |

The chosen value for C was slightly under the average from the measured capacitances, although taking 1.32 pF as an outlier value, then the proposed capacitance is reasonable. After plugging these values into (Equation 3 main text), we arrive at the following equation describing our current noise:

$$\sigma_{Res} = \sqrt{\frac{3.6\text{x}10^{-24}R^2 + 5.3\text{x}10^{-18}R + 1.6\text{x}10^{-11}}{R^2 + 31000R + 2.4\text{x}10^6}}$$

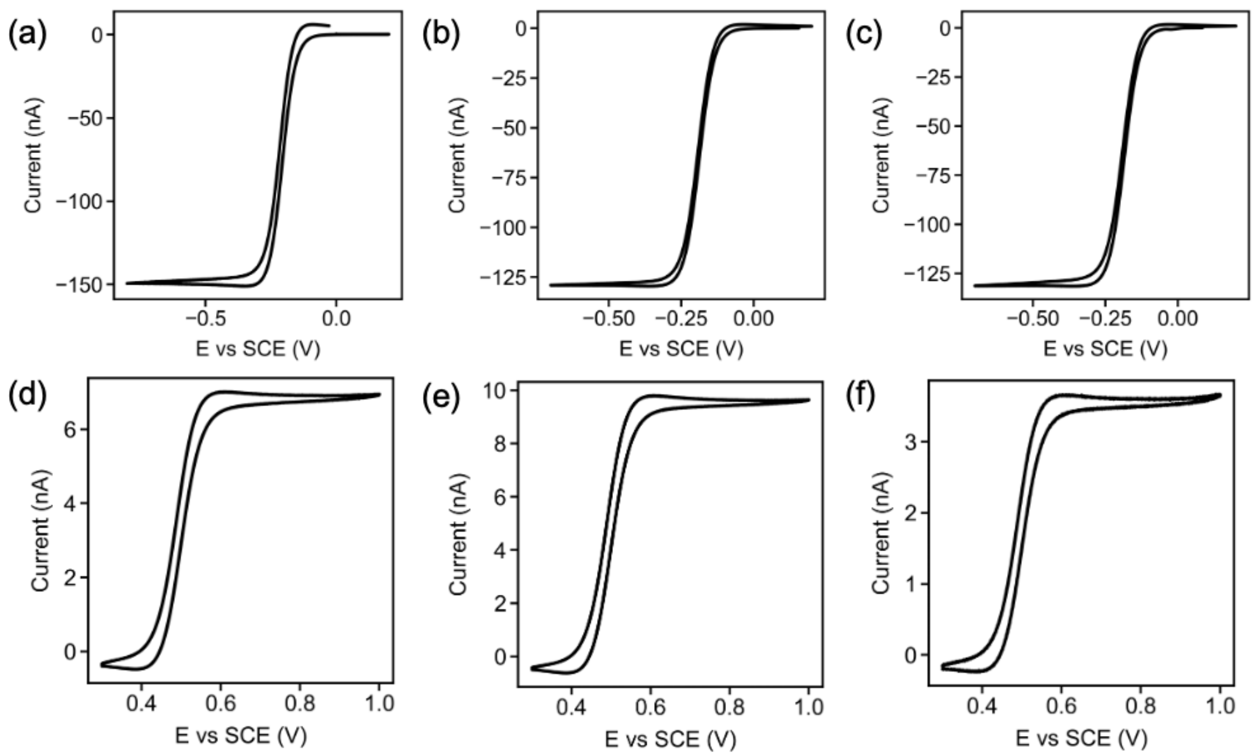


**Figure S2. Measured CVs of both [Ru($NH_3$)$_6$$Cl_3$] and TEMPO.** CVs of varying [Ru($NH_3$)$_6$$Cl_3$] concentrations ((a) 102.50 mM, (b) 80.18 mM, (c) 79.88 mM, 1 M [KCl], sparged with Ar gas) and varying TEMPO concentrations ((d) 5.02 mM, (e) 4.11 mM, (f) 5.70 mM, 50 mM sodium carbonate–sodium bicarbonate buffer) at the carbon fiber microelectrode. The CVs were used to calculate the diffusion coefficients of [Ru($NH_3$)$_6$$Cl_3$] and TEMPO in the following calculations.

**Calculations for the Diffusion Coefficient of Redox Probes**

The electrochemically active surface area of the electrode is determined using the steady-state current equation for a disk microelectrode.[1] Where $n$ is the number of electrons in the process, $F$ is Faraday's constant ($\mathrm{C\ mol^{-1}}$), $D$ is the diffusion coefficient ($\mathrm{m^2\ s^{-1}}$), $[C]$ is the bulk concentration of redox probe ($\mathrm{mol\ m^{-3}}$), and $r_e$ is the radius of the microelectrode (m).

$$i_{ss} = 4nFD[C]r_e$$

Using the measured currents and solving for the radius we yield.

$[Ru(NH_3)_6Cl_3]$ has a molar mass of 309.61 $\mathrm{g\ mol^{-1}}$ while TEMPO has a molar mass of 156.25 $\mathrm{g\ mol^{-1}}$. We will use the assumed radius provided from the supplier, BASI, of 5.5 μm.

**Table S3.** Calculated diffusion coefficient for $[Ru(NH_3)_6Cl_3]$

| Concentration (mM) | Observed Current (nA) | Calculated diffusion coefficient ($cm^2/s$) |
|---|---|---|
| 102.50 | -150.35 | 6.91 x $10^{-6}$ |
| 80.18 | -129.27 | 7.59 x $10^{-6}$ |
| 79.88 | -131.28 | 7.74 x $10^{-6}$ |

Reported $[Ru(NH_3)_6Cl_3]$ diffusion coefficient = $(7.41 \pm 0.36)$ x $10^{-6}$ $\mathrm{cm^2/s}$

**Table S4.** Calculated diffusion coefficient for TEMPO

| Concentration (mM) | Observed Current (nA) | Calculated diffusion coefficient ($cm^2/s$) |
|---|---|---|
| 4.11 | 6.97 | 7.99 x $10^{-6}$ |
| 5.70 | 9.74 | 8.05 x $10^{-6}$ |
| 2.06 | 3.58 | 8.19 x $10^{-6}$ |

Reported TEMPO diffusion coefficient = $(8.08 \pm 0.08)$ x $10^{-6}$ $\mathrm{cm^2/s}$

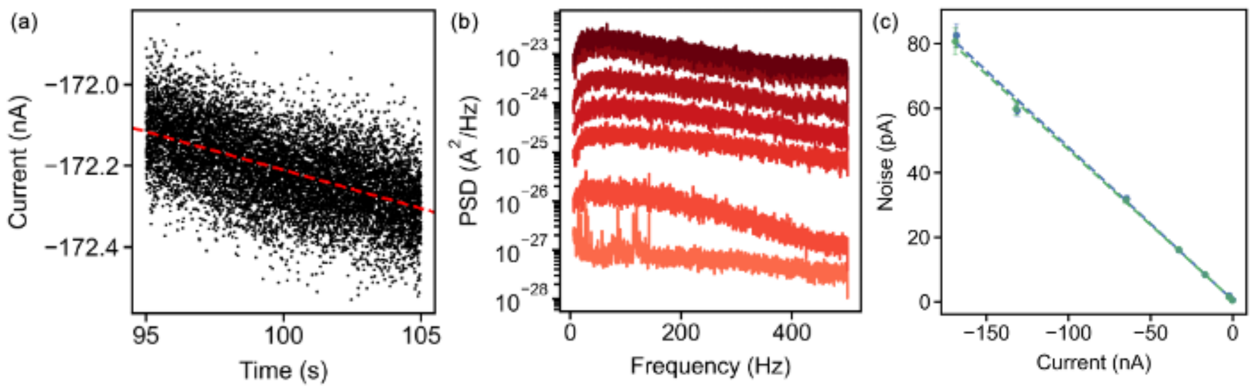


**Figure S3. Calculated current noise comparison via the root-mean square method (RMSE) and by using the power spectral density (PSD) to calculate noise.** (a) Example data set used in calculation of current noise using RMSE (0-100 mM [$Ru(NH_3)_6Cl_3$], 10 mM [KCl], sparged with Ar gas). (b) Example PSD plots of [$Ru(NH_3)_6Cl_3$] from 0-100 mM pre-processing to current noise (10 mM [KCl], sparged with Ar gas). (c) Direct comparison of the noise versus current plot from the two methods in (a) and (b) where green was calculated via PSD and blue was calculated via RMSE.

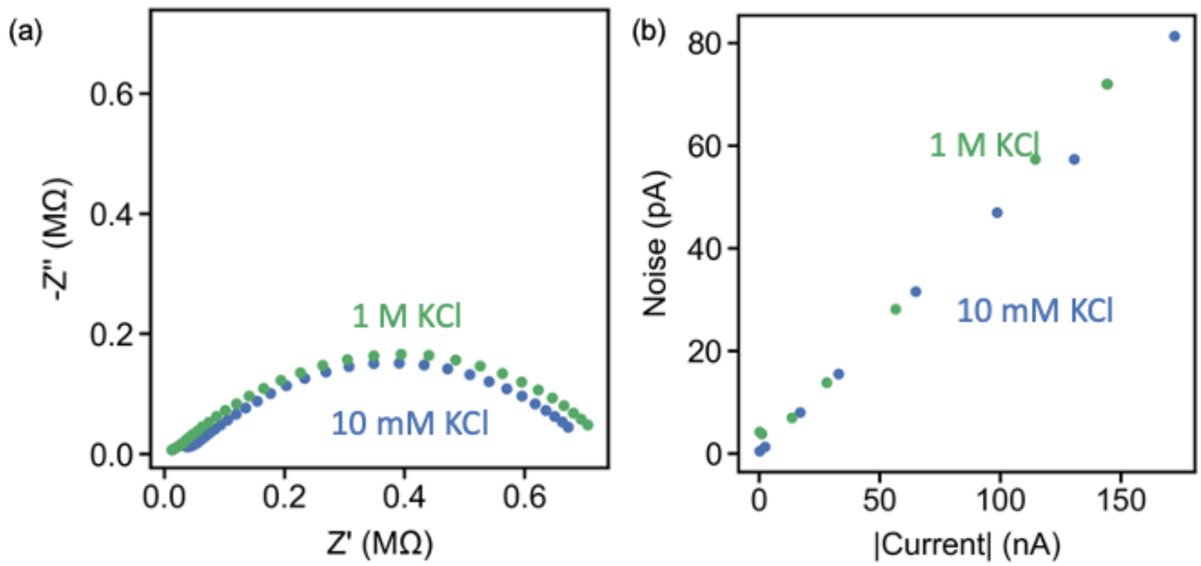


**Figure S4. Noise does not depend on electrolyte concentration.** (a) Nyquist plots of a 100 mM [$Ru(NH_3)_6Cl_3$] containing 1 M [KCl] versus 100 mM [$Ru(NH_3)_6Cl_3$] containing 10 mM [KCl]. (b) Calculated noise for a variety of [$Ru(NH_3)_6Cl_3$] concentrations at both electrolyte concentrations.

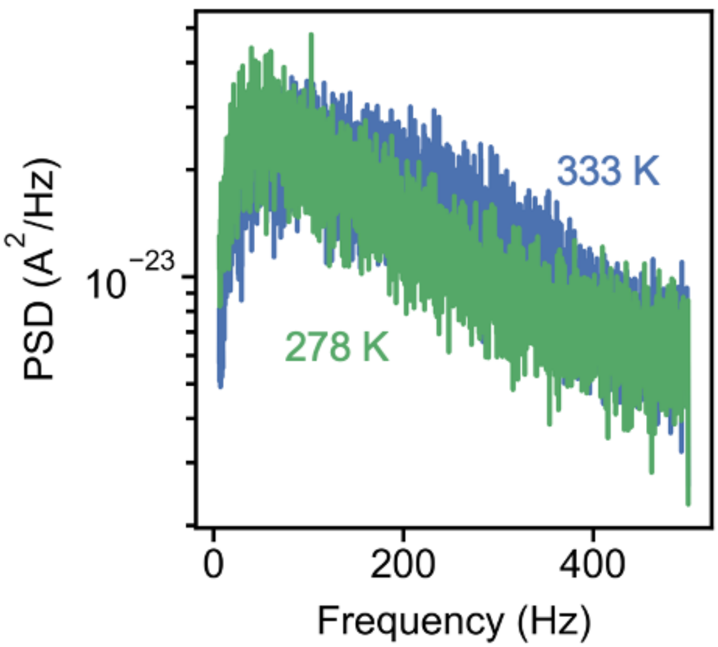


**Figure S5. The change in current noise at different temperatures is minimal, as expected from the Johnson−Nyquist equation.** PSD plots were calculated for two different temperatures, 278 K and 333 K, at 100 mM [$Ru(NH_3)_6Cl_3$] (1 M [KCl], sparged with Ar gas).

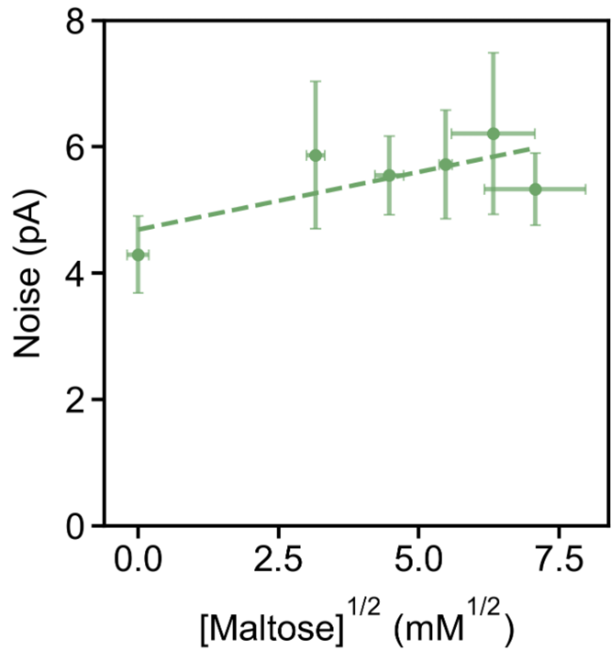


**Figure S6. Noise during an EC' reaction does not correlate with the square root of the mediator concentration.** RMS noise (pA) vs $[\text{Maltose}]^{1/2}$ $(\text{mM})^{1/2}$ for the maltose amplified TEMPO system (5 mM TEMPO; 0, 10, 20, 30, 40, and 50 mM maltose; 50 mM sodium carbonate−sodium bicarbonate buffer). A linear fit was performed ($R^2 = 0.504$).

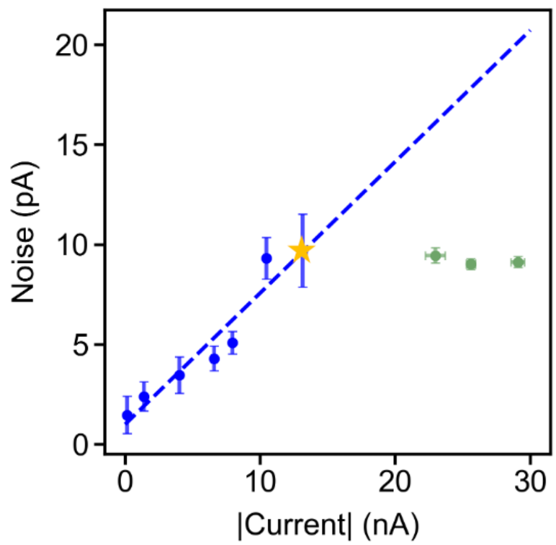


**Figure S7. At higher currents, EC' noise is still invariant of current.** RMS noise (pA) vs current (nA) for the maltose amplified TEMPO system (10 mM TEMPO; 10, 30, and 50 mM maltose, 50 mM sodium carbonate–sodium bicarbonate buffer). The star is 0 mM maltose, and the green points correspond to 10 – 50 mM maltose. The data is plotted against the linear fit for the TEMPO without maltose system (dashed, blue line) which has been extrapolated to higher currents along with the original TEMPO data without maltose (blue).

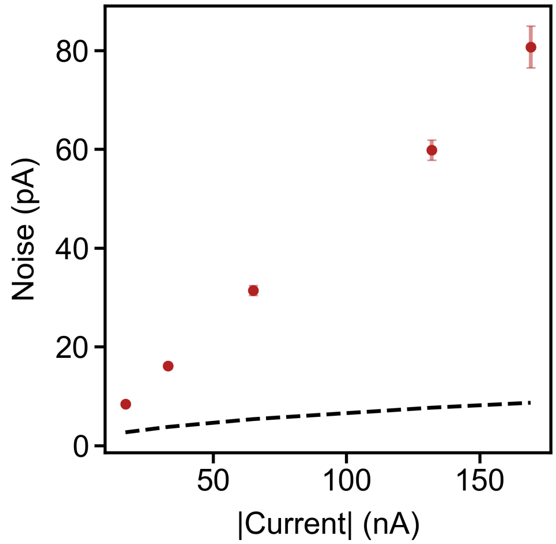


**Figure S8. Noise at a microelectrode is not dictated by classical shot or thermal noise phenomenon.** Noise (pA) versus current (nA) for the [Ru($NH_3$)$_6$$Cl_3$] system (red, circles, 0 – 100 mM [Ru($NH_3$)$_6$$Cl_3$], 10 mM [KCl], sparged with Ar gas) plotted against the total, calculated noise stemming from the classical definitions of shot and thermal noises (black, dashed).

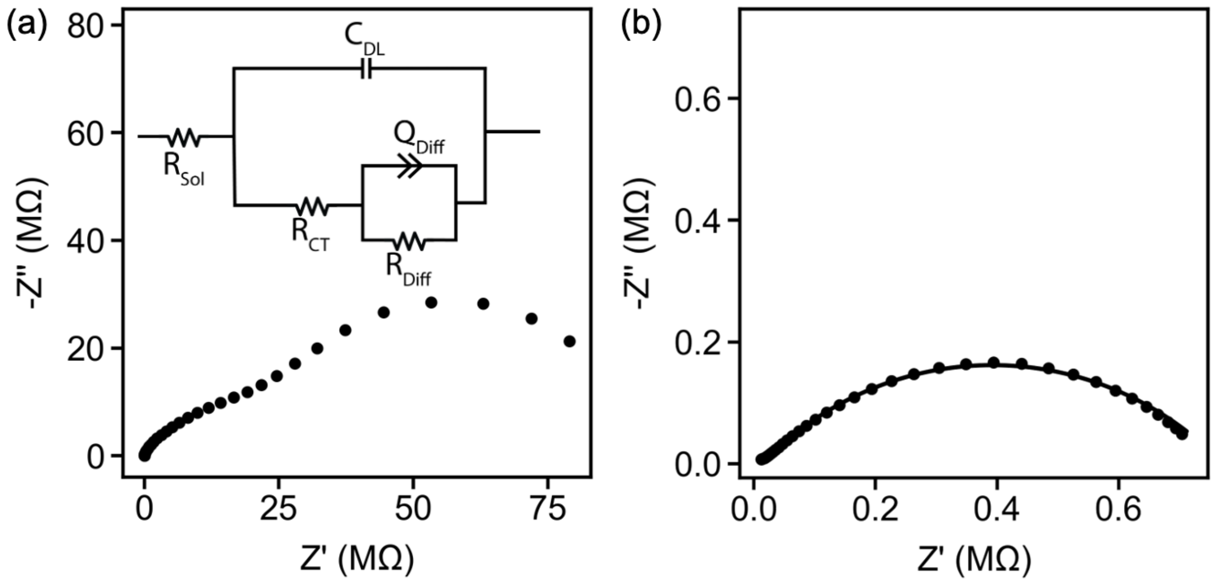


**Figure S9. Charge transfer resistance at a microelectrode is only observable at low redox probe concentrations.**[2] Electrochemical impedance spectra (100 kHz to 100 mHz) at (a) 1 mM [$Ru(NH_3)_6Cl_3$] (1 M [KCl], sparged with Ar gas) and (b) 100 mM [$Ru(NH_3)_6Cl_3$] (1 M [KCl], sparged with Ar gas).

**Table S5.** EIS Fit Parameters for $[Ru(NH_3)_6Cl_3]$ EIS – 1 M [KCl]

| Concentration (mM) | $R_{Diff}$ (MΩ) | $Q(F^{1/\alpha}\,s^{(\alpha-1)})$ | $\alpha$ |
|---|---|---|---|
| 10 | 8.26 | $2.45 \times 10^{-8}$ | 0.512 |
| 20 | 4.09 | $4.34 \times 10^{-8}$ | 0.509 |
| 40 | 1.98 | $7.88 \times 10^{-8}$ | 0.511 |
| 60 | 1.28 | $1.19 \times 10^{-7}$ | 0.510 |
| 80 | 0.96 | $1.54 \times 10^{-7}$ | 0.511 |
| 100 | 0.76 | $1.91 \times 10^{-7}$ | 0.514 |

**Table S6.** EIS Fit Parameters for TEMPO EIS – 50 mM Carbonate Buffer

| Concentration (mM) | $R_{Diff}$ (MΩ) | $Q(F^{1/\alpha}\,s^{(\alpha-1)})$ | $\alpha$ |
|---|---|---|---|
| 5 | 15.63 | $9.94 \times 10^{-9}$ | 0.578 |
| 8 | 10.10 | $1.27 \times 10^{-8}$ | 0.568 |
| 10 | 8.22 | $2.17 \times 10^{-8}$ | 0.526 |

**Table S7.** EIS Fit Parameters for TEMPO–Maltose EIS – 50 mM Carbonate Buffer

| Concentration Maltose (M) | $R_{Diff}$ (MΩ) | $Q(F^{1/\alpha}\,s^{(\alpha-1)})$ | $\alpha$ |
|---|---|---|---|
| 10 | 13.50 | $6.47 \times 10^{-9}$ | 0.619 |
| 20 | 12.55 | $4.19 \times 10^{-9}$ | 0.638 |
| 30 | 12.98 | $4.52 \times 10^{-9}$ | 0.616 |
| 40 | 13.01 | $3.46 \times 10^{-9}$ | 0.641 |

**The constant phase element is that of diffusion, not of double layer capacitance.**

The double layer should act as that of an ideal capacitor with a phase of about 90° while a diffusional, Warburg-like, element would expect a phase closer to 45°. In impedance modeling, this corresponds to $\alpha$ values in a constant phase element of 1 for the former and 0.5 for the latter.

## REFERENCES


(1) Bard, A. J.; Faulkner, L. R. *Electrochemical Methods: Fundamentals and Applications*, 2nd ed.; Wiley: New York, 2001.

(2) Abrantes, L. M.; Fleischmann, M.; Peter, L. M.; Pons, S.; Scharifker, B. R. On the Diffusional Impedance of Microdisc Electrodes. *J. Electroanal. Chem. Interfacial Electrochem.* **1988**, *256* (1), 229–233. https://doi.org/10.1016/0022-0728(88)85023-X.